Prediction Models of Tumor Growth Trajectories Based on Pretreatment CT Images of TKI-Treated Lung Cancer Patients

Huy Gia Truong
Kyushu University
Hidetaka Arimura (arimurah@med.kyushu-u.ac.jp)
Kyushu University
Kentaro Tanaka
Kyushu University Hospital
Kenta Ninomiya
Kyushu University
Quoc Cuong Le
Kyushu University

Research Article

Keywords: TGTs, NSCLC, TKI, cancer

Posted Date: February 22nd, 2021

DOI: https://doi.org/10.21203/rs.3.rs-196528/v1

Confidential until publication in Scientific Report

Prediction Models of Tumor Growth Trajectories Based on Pretreatment CT Images of TKI-treated Lung Cancer Patients

Authors:

Huy Gia Truong[1], Hidetaka Arimura[2*], Kentaro Tanaka[3*], Kenta Ninomiya[1], Quoc Cuong Le[1]

Affiliations:

[1] Division of Medical Quantum Science, Department of Health Sciences, Graduate School of Medical Sciences, Kyushu University

[2] Division of Medical Quantum Science, Department of Health Sciences, Faculty of Medical Sciences, Kyushu University

[3] Respiratory Medicine, Kyushu University Hospital

Corresponding authors:

Hidetaka Arimura, PhD, Division of Medical Quantum Science, Department of Health Sciences, Faculty of Medical Sciences, Kyushu University, 3-1-1, Maidashi, Higashi-ku, Fukuoka 812-8582, Japan

[E-mail: arimurah@med.kyushu-u.ac.jp]

Kentaro Tanaka, MD, PhD, Department of Respiratory Medicine, Kyushu University Hospital, 3-1-1, Maidashi, Higashi-ku, Fukuoka 812-8582, Japan

[E-mail: tanaka-k@kokyu.med.kyushu-u.ac.jp]

Summary (193/200 words)

We have developed prediction models of tumor growth trajectories (TGTs) based on pretreatment computed tomography (CT) images, prior to targeted therapy with four specific tyrosine kinase inhibitors (TKIs)—erlotinib, gefitinib, afatinib, and osimertinib—for epidermal growth factor receptor (EGFR)-mutated non–small-cell lung carcinoma (NSCLC) patients. TGTs of the time-variant number of tumor cells were predicted for individual patients with tumor growth equations under the assumption that each tumor could contain three cell types: TKI drug-sensitive, drug-persister, and drug-resistant populations. Seven parameters of the TGT models were estimated by support vector regression, which learned the relationships between principal component features and the referenced parameters that were optimized by a Levenberg–Marquardt method. The Spearman correlation coefficient was employed to evaluate the correlation in the number of tumor cells at each CT acquisition timepoint between the reference numbers (derived from CT images) and predicted numbers. The average Spearman correlation was 0.822 (p=0.073) for a training dataset (27 treatments) and 0.818 (p=0.042) for a test dataset (10 treatments). The proposed models could predict TGTs for TKI non-treated patients, thereby estimating how lung tumors will respond to specific TKI drugs to optimize the selection of treatment strategies.

Introduction

Lung cancer is the commonest malignant cancer (11.6% of the total cancer cases) worldwide, with an associated mortality rate of 18.4%[1]. Targeted therapy with tyrosine kinase inhibitors (TKIs) is the most efficient treatment modality for controlling tumor growth in stage III or IV non–small cell lung carcinoma (NSCLC), which accounts for more than 80% of lung cancer cases[2]. TKIs mainly target the epidermal growth factor receptor (EGFR) inside the tumor to block the growth factor signal, thereby causing tumor cells to die. Unfortunately, tumor response to first-line agents, which includes first- and second-generation TKIs such as erlotinib, gefitinib, and afatinib, is unexpectedly weakened within 10–12 months. This is because of the emergence of TKI-resistant cells due to the secondary EGFR mutation *T790M*, which appears in more than half of all cases[3]. Therefore, the second-line TKI, osimertinib (third-generation TKI), should be applied in a timely manner for patients who make the transition from complete/partial response (CR/PR) to stable/progressive disease (SD/PD). However, there are two challenging issues, as follows: (1) the prediction of the tumor response to specific TKI drugs (e.g., CR/PR or SD/PD); and (2) the prediction of the transition period from the CR/PR to PD. One of approaches to solve this problem would be the prediction of the tumor growth trajectories (TGTs) with regard to time, and this approach could improve the selection of lung cancer treatment strategies prior to targeted TKI therapies.

Studies on the estimation of TGTs after targeted TKI therapies for EGFR-mutated NSCLC patients[4,5,6,7]. Michor et al.[4] developed a mathematical model which describes the four layers of the differentiation hierarchy of the hematopoietic system in NSCLC patients with chronic myeloid leukemia treated by breakpoint cluster region-abelson (BCR-ABL) TKI-imatinib. The authors calculated the probability of developing imatinib resistance (*BCR-ABL*) mutations and estimated

the time until the detection of resistance, thereby providing the first quantitative insights into the in vivo kinetics of a human cancer. Foo et al.[5], in contrast, constructed a simple mathematical model using birth and death processes to describe the evolution of resistant cells during a targeted anticancer therapy for NSCLC patients. Their model aimed to develop a methodology for designing optimal drug administration strategies to minimize the risk of resistance in clinical practice. With an effort to discover the emergence of resistance factors, Mumenthaler et al.[6] investigated the effect of local microenvironmental factors such as drug concentration, oxygen, and glucose on the evolution of erlotinib-resistant cells by exposing the same cancer cells (either drug-sensitive or drug-resistant) to specified conditions for observing the changes in cell behaviors in terms of growth and response to the therapy. In each microenvironmental factor, a multitype time-inhomogeneous stochastic branching process model was developed to describe the population of cancer cells. By considering the abnormal growth of post-treatment resistant population caused by *T790M* mutation, Grassberger et al.[7] applied a mathematical Gompertz growth equation combined with a cell loss model to describe the TGTs for a TKI (erlotinib) treatment by using tumor volume data calculated from pretreatment and post-treatment computed tomography (CT) images. In Grassberger's study, the assumption was that the lung cancer tumor contains three types of cell components: TKI drug-sensitive cells, which can be killed by TKIs; TKI drug-resistant cells, which are resistant to TKIs; and drug-tolerant persister cells, which can potentially mutate into resistant cells via a *T790M* mutation. Accordingly, Grassberger successfully estimated the initial fraction of persister and resistant populations to administer treatment strategies.

The numbers of cancer cells estimated both before and after the targeted TKI therapy were required to predict the TGTs in earlier studies and, therefore, TGTs for new NSCLC patients

cannot be predicted prior to the TKI therapy using the abovementioned approaches. Meanwhile, prediction models of tumor responses before the application of TKIs have been increasingly demanded for the timely selection of a more appropriate treatment strategy for each patient.

Therefore, in this study, we developed prediction models of TGTs to estimate the responses of NSCLC tumors based on pretreatment CT images obtained before TKI (i.e., erlotinib, gefitinib, afatinib, and osimertinib) treatment. We hypothesized that quantitative imaging features ascertained from pretreatment CT images can determine the TGT models for individual patients.

Results

The prediction models of TGTs developed in this study is described in Fig. 1, wherein support vector regression (SVR) is used, because the SVR showed the best results for the prediction of TGTs among two machine learning models, that is, the SVR and random forest (RF), in this study.

In this approach, the input information comprised the pretreatment CT images and the name of the TKI. Tumor contours were manually delineated on the pretreatment CT images. Initial tumor volumes and image features were calculated from those segmented tumor regions. In total, 486 image features calculated from the pretreatment CT images were summarized into three principal component (PC) features by reducing the original dimension using principal component analysis (PCA). Seven parameters in the TGTs model were automatically determined by using the SVR, which learned the relationships between the PC features and the referenced parameters that were optimized using a Levenberg–Marquardt method. The TGT models of time-variant number of tumor cells were predicted according to a Gompertz tumor growth model that was combined with a cell loss model under the assumption that each tumor could contain three cell types, that is, sensitive, persister, and resistant populations, which have different responses to TKIs.

The evaluation metrics in this study included a Spearman correlation coefficient and the mean absolute percentage error (MAPE) between the number of tumor cells derived from tumor volumes (CT images) and the predicted number of tumor cells predicted by the TGT model. The Spearman correlation coefficient can assess the tumor growth tendency, such as a transition from CR/PR to SD/PD.

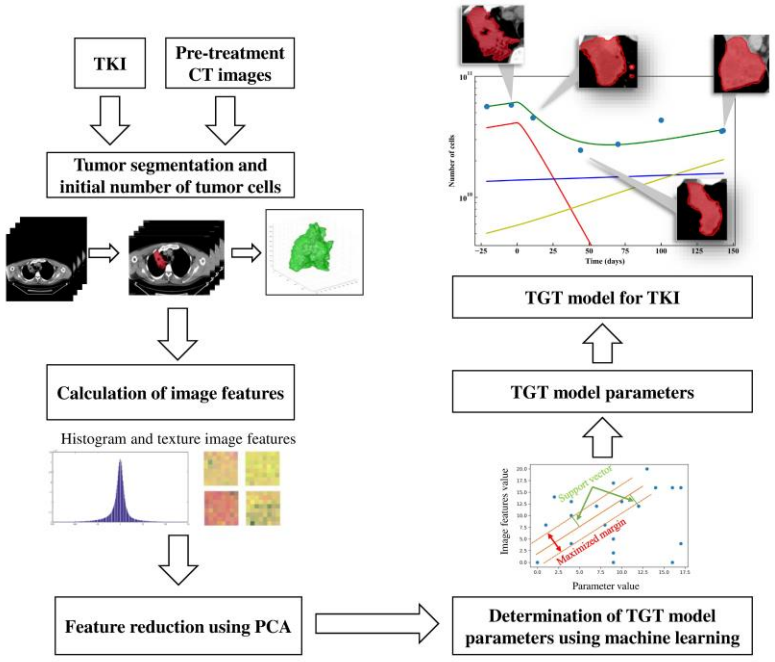

Figure 1. A scheme for the prediction of TGT models. TKI: tyrosine kinase inhibitor, PCA: principal component analysis, TGT: tumor growth trajectory.

Figure 2(b) shows the TGTs of a representative patient who was treated with afatinib in a test dataset. The actual lung tumor regions of interest (ROIs; red) on the pretreatment and follow-up CT images at four CT acquisition times (A, B, C, and D) on the TGTs are illustrated in Fig. 2(a). The three components, drug-sensitive, drug-tolerant-persister, and drug-resistant cells, and the total number of tumor cells are indicated by red, blue, and yellow and a green solid line, respectively; the number of tumor cells derived from CT images, which was used as the reference,

is indicated by a blue circle. In this patient, a very high correlation between the reference and predicted number of tumor cells was showed. The TGT model predicted results with a Spearman correlation of 0.905 (p=0.002) and an MAPE of 8.12%.

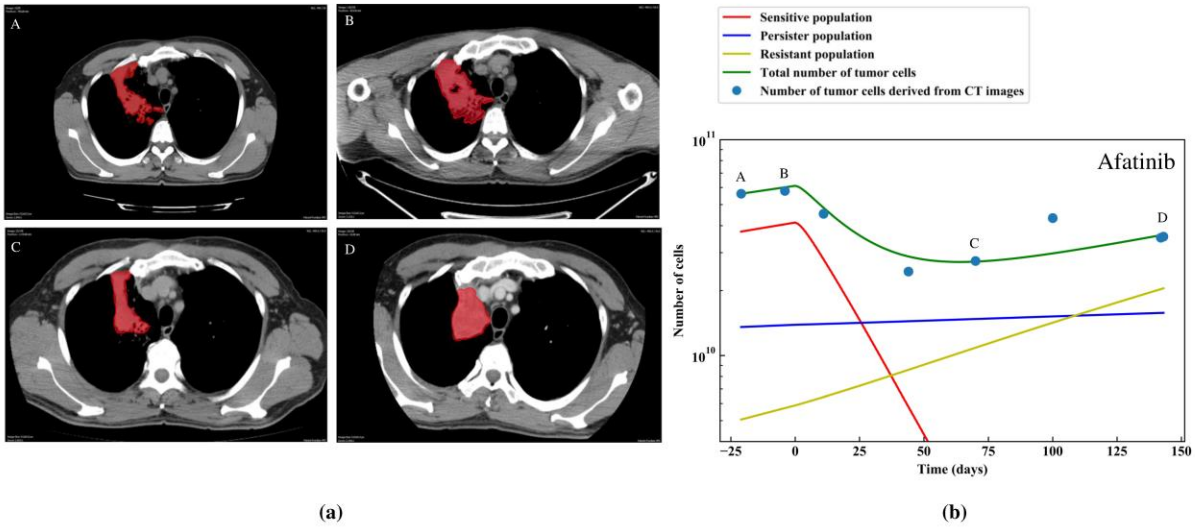

Figure 2. TGTs of a patient treated with afatinib in a test dataset: (a) actual lung tumor ROIs (red) on the pretreatment and follow-up CT images at four CT acquisition timepoints (A, B, C, and D) on the TGTs and (b) the predicted TGTs with the number of tumor cells derived from the CT images (solid circles).

Furthermore, the proposed model has the ability to predict various types of tumor responses to TKI treatments. As shown in Fig. 3, there were three common types of treatment outcomes in this study: (a) PR to SD, (b) PR to PD, and (c) PD.

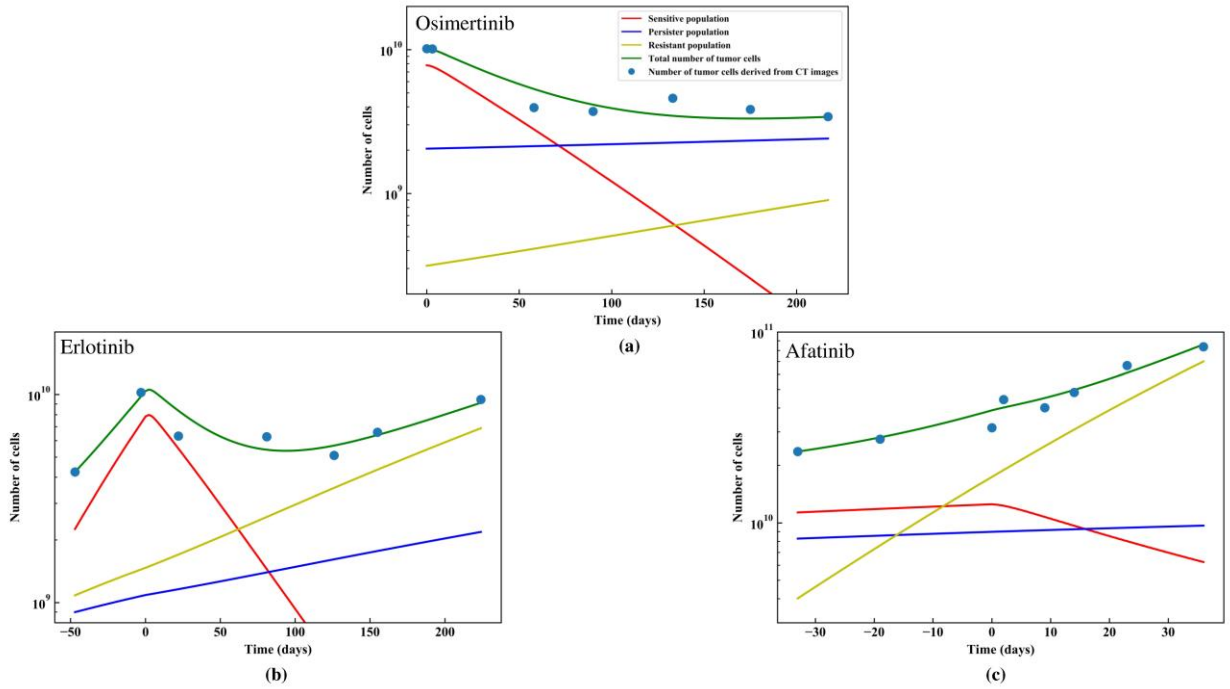

Figure 3. Three common types of TGTs: (a) PR to SD, (b) PR to PD, and (c) PD. PR: partial response, SD: stable disease, PD: progressive disease.

Figure 4 shows the box plot charts of the Spearman correlation and the MAPE between the number of tumor cells derived from CT images and predicted number of tumor cells ascertained by the proposed model in training and test datasets. In total, there were four independent groups of TKI-specific treatments (total treatments, 27) in the training dataset as follows: 4, 7, 8, and 8 treatments in the erlotinib, afatinib, gefitinib, and osimertinib groups, respectively. The average Spearman correlation between the number of tumor cells derived from CT images and the number of tumor cells predicted by the proposed model was 0.822 (p=0.073) for a training dataset with an average MAPE of 13.6% (Supplementary Table S1). The SVR model showed a better result than the RF model (average Spearman correlation: 0.586; p=0.231; average MAPE: 97.4%; Supplementary Table S2).

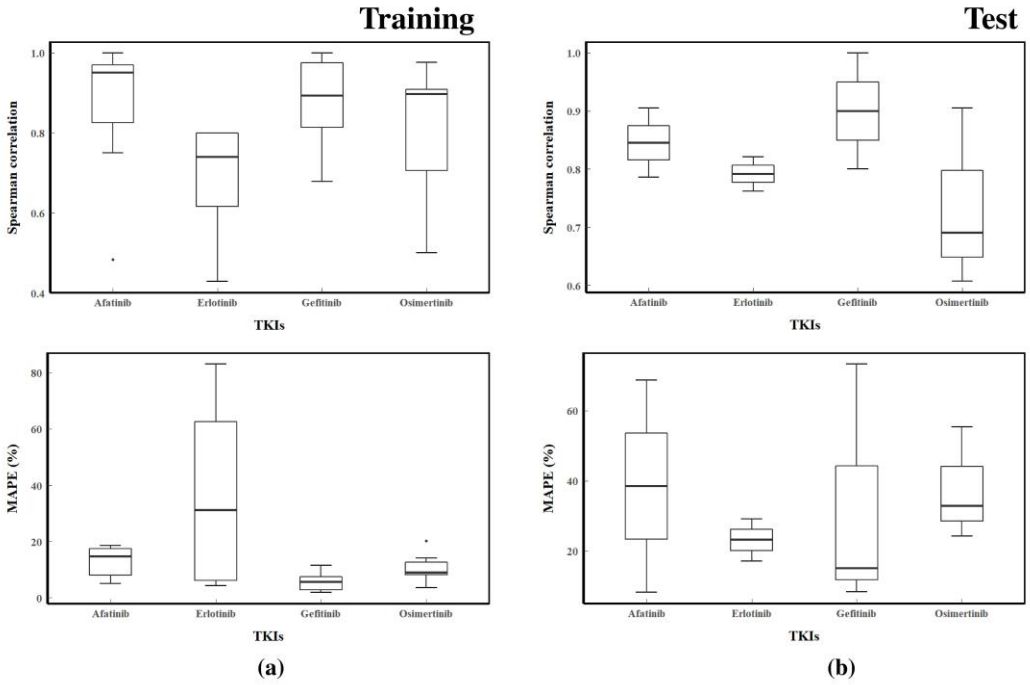

Figure 4. The box plot charts: (a) Spearman correlation and MAPE between the number of tumor cells derived from CT images and the number of tumor cells predicted by the TGT model in a training dataset; (b) Spearman correlation and MAPE between number of tumor cells derived from CT images and the predicted number of tumor cells estimated by a TGT model in a test dataset. TGTs: tumor growth trajectories, MAPE: mean absolute percentage error.

In Fig. 4(a) of a training dataset, the Spearman correlation for the erlotinib, afatinib, gefitinib, and osimertinib groups was 0.677 (p=0.208; MAPE 37.4%), 0.861 (p=0.035; MAPE 12.7%), 0.879 (p=0.028; MAPE 5.65%), and 0.803 (p=0.083; MAPE 10.5%), respectively.

Figure 4(b) shows the Spearman correlation and MAPE in a test dataset (Supplementary Table S3) which accounted for 10 treatments as follows: 2, 2, 3, and 3 treatments in the erlotinib, afatinib, gefitinib, and osimertinib groups, respectively, with an overall average Spearman correlation of 0.818 (p=0.042) with a MAPE of 33.2%. Furthermore, the SVR model performed

better than the RF model (overall average Spearman correlation: 0.652, p=0.166, with a MAPE of 43.5%; Supplementary Table S4).

The Spearman correlation in the erlotinib, afatinib, gefitinib, and osimertinib groups was 0.792 (p=0.026; average MAPE 23.1%), 0.845 (p=0.011; average MAPE 38.5%), 0.900 (p=0.047; average MAPE 32.2%), and 0.734 (p=0.069; average MAPE 37.5%), respectively.

Discussion

The proposed model showed a suitable potential for predicting the tendency of TGTs of patients who were treated with TKIs or their combinations based on the pretreatment CT images. Tumor response prediction prior to the initiation of TKI treatment could increase precision of TKI selection as well as selection of timepoints for switching to a different TKI during the treatment in clinical practice.

The pretreatment CT images to calculate the imaging features evaluated in this study were obtained using four scanners made by different manufacturers in Kyushu University Hospital (KUH) as follows: GE Medical (10 treatments, PET/CT), Toshiba (16 treatments), Philips (7 treatments), and Siemens (4 treatments) (Table 3). In clinical practice at the study center, lung cancer is diagnosed mainly based on conventional CT images that have a higher image quality (resolution and noise) rather than on CT images in PET/CT scanners. Despite the use of different types of CT scanners to obtain the pretreatment images, we predicted TGTs with relatively high correlations. Therefore, the proposed model may have the robustness to predict the TGT whereas overcoming the different imaging qualities of multiple CT scanners.

Earlier studies included patients with the *T790M* mutation, whereas this study cohort comprised participants with *19del*, *L858R*, and *T790M* mutations who were treated with targeted TKI therapy under a defined clinical protocol. Other mutations and wild-type lesions were excluded from this study. Nonetheless, the proposed model can be applied to other mutation types, such as *ALK*, *KRAS*, *BRAF*, and so on. Further studies are needed to extend the application of the model to hematological malignancies.

We developed TGT prediction models for four TKIs—erlotinib, gefitinib, afatinib, and osimertinib—that have been specified for NSCLC EGFR-mutation treatments. It is necessary to apply the proposed model for other drugs approved by drug administration offices, such as the Food and Drug Administration, for other mutations in NSCLC patients. We believe that this approach will validate the TGT prediction methods for managing the targeted TKI therapeutic strategies.

This study has two main limitations. First, the number of patients included in this study was small. The total number of patients from both the training and test datasets was 24, which was larger than that in an earlier study[7] (17 patients). The proposed model could predict the tumor growth tendencies during the specific TKI treatments with average Spearman correlation coefficients of 0.822 and 0.818 in training and test datasets, respectively, although average MAPEs of 13.6% (training) and 33.2% (test) were reported. These large errors could be reduced by increasing the number of patients. Second, the primary criterion for selecting the patient cohort was patients with only targeted TKI therapy during the treatment duration. However, the combination of targeted therapy with other treatment modalities, such as radiation therapy or chemotherapy, has been proved to ensure the best treatment outcomes.[8,9] Therefore, we suggest that future studies should develop strategies for prediction of complete tumor responses after

combination treatment to provide physicians with more complete and appropriate information for treatment selection. We believe that this is a potential subject for our future research.

Conclusions

The TGT models for predicting the tumor response to specific TKI drugs using pretreatment CT could predict TGTs for non-TKI-treated patients, thereby facilitating the estimation of how lung tumors will respond to specific TKI drugs to enable the selection of optimal treatment strategies.

Methods

Clinical data

The study protocol was approved by the Kyushu University Certified Institutional Review Boards for Clinical Trials, and informed consent waiver was granted because this research was a retrospective study. We confirmed that all methods were performed in accordance with the relevant guidelines and regulations of the institutional review boards. The patient information is summarized in Table 1. There were 24 patients with 37 treatments who were selected from 100 NSCLC patients in the KUH patient database based on the study eligibility criteria. We mainly focused on solid NSCLC tumors which had three EGFR mutation subtypes: *L858R* (8 patients), *19del* (13 patients), and *T790M* (3 patients). With an age range of 33 to 85 years (average 72 years), 2, 10, 6, and 6 patients were diagnosed with stages I, II, III, and IV NSCLC, respectively. The patients received TKI treatments only during the treatment durations, which ranged from 36 to 412 days (average 204 days).

Table 1. Clinical characteristics of the patients.

Information	**Value**
Number of patients	24
Number of treatments	37
Age	33 – 85 years (average: 72 years)
Gender	14 females, 10 males
Tumor stage	
• Stage I	2 patients
• Stage II	10 patients
• Stage III	6 patients
• Stage IV	6 patients
Treatment duration	36 – 412 days (average: 204 days)
Initial tumor volume	1.25 – 201 cm^3 (average: 44.8 cm^3)
Number of cells in first CT acquisition	3.50×10^8 – 5.62×10^{10} cells (average: 1.25×10^{10} cells)

From the original matrix sizes of the pretreatment CT images (512 × 512 × 46 – 456, median: 153) and pixel size (from 0.429 × 0.429 mm^2 to 0.977 × 0.977 mm^2, median: 0.743 × 0.743 mm^2), radiotherapy (RT)-structure images after ROI segmentation were converted to binary images and transformed into isotropic images using a shape-based interpolation.[10] In accordance with the various original pixel sizes (0.625 × 0.625 mm^2), we set an iso-voxel size of 0.625 × 0.625 × 0.625 mm^3. The number of iso-voxels inside the ROIs was counted and the number was multiplied with the unit volume of an iso-voxel for obtaining tumor volumes. The initial tumor

volumes were measured from the very first CT acquisitions ranged from 1.25 to 201 cm^3 (average 44.8 cm^3). Furthermore, the initial number of tumor cells was derived by multiplying the tumor volume with 2.8×10^8 cells/cm^3.[7]

Four specific TKIs were used in this study: erlotinib, gefitinib, afatinib, and osimertinib. Drugs characteristics, such as the dose, half-life, and maximum concentration, at steady state for each TKI are listed in Table 2.[3]

Table 2. TKI drug information and characteristics.

Name of drug	Osimeritinib	Gefitinib	Afatinib	Erlotinib
Dose (mg / day)	80	250	40	150
Drug half-life (hours)	48.6	52.0	37.0	36.0
Maximum concentration at steady state (μg / mL)	0.328	0.101	3.80×10^{-2}	1.52

Table 3 shows the treatment and its related information in the training and test datasets. The study cohort was divided into four groups of specific TKI treatments. Each TKI group was then randomly subdivided into two groups, the training dataset (80%) and test dataset (20%), to develop four independent TGT models for the four TKI groups (Supplementary Fig. S1).

Ten patients had 2 or 3 tumor regions, which were named GTV1, GTV2, and GTV3. Therefore, those patients received 2 or 3 specific TKI treatments, which were the first, second, and third treatments. That is because patient IDs were overlapped in both training (20 patients) and test (7 patients) datasets (Supplement Tables S1-S4).

Table 3. Treatment and its related information in the training and test datasets.

Information	No. of treatments		
	Total	**Training dataset**	**Test dataset**
Number of treatments	37	27	10
NSCLC subtypes			
• Adenocarcinoma	34	25	9
• Squamous cell carcinoma	1	1	0
• Non-defined	2	1	1
Mutant type			
• L858R	13	7	6
• 19del	20	16	4
• 19del/T790M	3	3	0
• L858R/T790M	1	1	0
TKI Treatments			
• Erlotinib	6	4	2
• Gefitinib	11	8	3
• Afatinib	9	7	2
• Osimertinib	11	8	3
Treatment outcomes			
• Partial response (PR)	4	4	0
• Progressive disease (PD)	6	5	1
• Stable disease (SD)	5	5	0
• PR to SD	14	8	6
• PR to PD	8	5	3

Pretreatment CT scanner manufacturers			
• GE Medical (CT in PET/CT)	10	8	2
• Toshiba	16	9	7
• Philips	7	6	1
• Siemens	4	4	0

Furthermore, tumor responses for TKI treatments were evaluated by using a volumetric response criteria[11,12]: PR (tumor volume decrease by 30%), PD (tumor volume increase by 20%), SD (neither the PR nor PD criteria are met), and PR to SD and PR to PD. The increase and decrease in tumor volume were calculated from before to after the treatment after at least 4 weeks for the evaluation of PR and CR at least 6–8 weeks for evaluation of SD.[13]

Tumor segmentation

The ROIs of all pretreatment and follow-up CT images were segmented using 3D Slicer software,[14] with a window width of 400 and a window level of 50 for soft tissue. The segmentations were supervised based on a consensus between a clinical doctor for lung cancer (KT) and a medical physicist (HA) with 8 years of experience in the field.

TGT models

Tumor growth could be described by several mathematical models[15]. The first preference was for an exponential model; however, from a biological perspective, the exponential model was unrealistic as it implied the tumor could grow until infinity despite the nutrient limitation in the

human body. Therefore, the Gompertz model was introduced, after adding the following upper limit: the tumor-carrying capacity was added to restrict the infinite-growth problem. Based on this idea, many models were subsequently proposed, including the Power Law model, Logistic model, Dynamic CC model, etc. Nevertheless, for evaluating the best TGT model, we used a statistical root mean square error (RMSE), which proved that the Gompertz model had the lowest error values compared to others[16].

Thus, under the assumption that each tumor could contain three types of cells, drug-sensitive (cells that could be killed by TKI drugs), drug-tolerant persister (cells that could mutate into resistant cells), and drug-resistant (cells that resist the effect of TKI drugs) cells, a TGT model (Fig. 5) was developed from the original Gompertz equation[17]:

$$\frac{dN(t)}{dt} = \lambda N(t)\log\left(\frac{K}{N(t)}\right) \tag{1}$$

where $N(t)$ was the total number of tumor cells at a timepoint t, λ was the growth rate parameter, and K was the tumor-carrying capacity, which was set to 4.09×10^{12} cells (constant) in this study[7]. Each cell population had their own Gompertz equation to describe their growth. In particular, for the drug-sensitive population, the Gompertz equation was combined with a cell loss model to describe the tumor shrinkage during TKI treatment as follows[7]:

$$\frac{dN(t)}{dt} = -\beta_c C(t) N(t) \tag{2}$$

with

$$C\,(t) = C_{max}\, e^{-\frac{ln(2)}{t_{1/2}}t} \tag{3}$$

where the $t_{1/2}$ (days) and C_{max} (μg/mL) were the half-life and maximum concentration in a steady state of TKI drugs, and β_c was the cell loss parameter. The values of the half-life and maximum

concentration depend on the specific TKI drugs listed in Table 2. Thus, a drug-sensitive population[7] was defined as:

$$\frac{dN_s}{dt} = \lambda_s N_s \log\left(\frac{K}{N_{total}}\right) - \beta_c C(t) \lambda_s N_s \log\left(\frac{K}{N_{total}}\right) \quad (4)$$

where N_s was the number of drug-sensitive cells, λ_s was the growth rate of sensitive cells, N_{total} was the total number of tumor cells. Similarly, a drug-tolerant persister population[7] was described by the subtraction of persister cells that mutate into resistant cells from persister cells to contribute to tumor growth as follows:

$$\frac{dN_P}{dt} = \lambda_P N_P \log\left(\frac{K}{N_{total}}\right) - \mu \lambda_P N_P \log\left(\frac{K}{N_{total}}\right) \quad (5)$$

where N_P was the number of persister cells, λ_P was the growth rate of persister cells, and μ was compound mutation probability. Simultaneously, the drug-resistant population[7] was expressed by:

$$\frac{dN_R}{dt} = \lambda_R N_R \log\left(\frac{K}{N_{total}}\right) + \mu \lambda_P N_P \log\left(\frac{K}{N_{total}}\right) \quad (6)$$

where N_R was the number of resistant cells and λ_R was the growth rate of resistant cells. The right side represents the sum of the resistant cells that contribute to tumor growth and the mutated cells from persister cells.

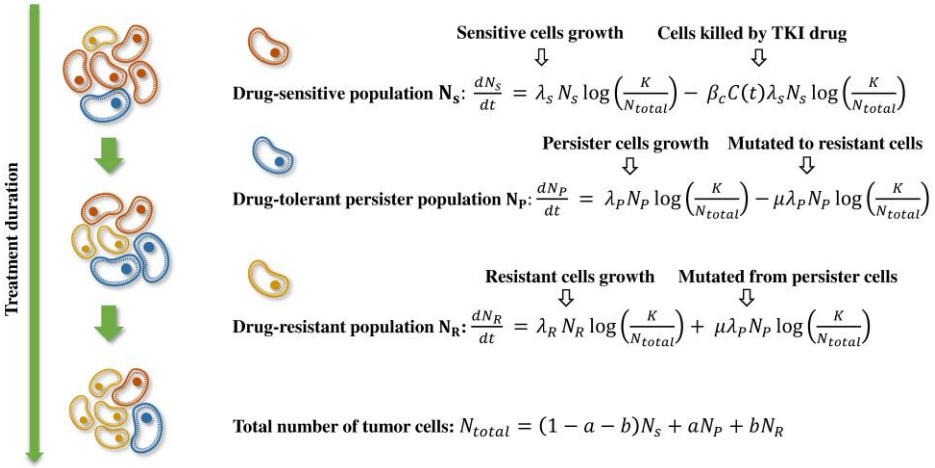

Figure 5. The TGT model of the time-variant number of tumor cells with the assumption that there are three components inside the NSCLC tumor: a drug-sensitive population, a drug-tolerant persister population, and a drug-resistant population

The total number of tumor cells was the sum of three cell populations with identical initial fractions of resistant and persister populations as follows:

$$N_{total} = (1 - a - b)N_s + aN_P + bN_R \tag{7}$$

where a was the initial fraction of the persister population and b was the initial fraction of the resistant population.

Determination of reference parameters in TGTs model using a Levenberg-Marquardt method

In total, seven parameters were employed in this TGT model: three growth rates of sensitive, persister, and resistant populations (λ_s, λ_P, and λ_R), the cell loss parameter (β_c), the compound

mutation probability (μ), and the initial fractions of persister and resistant populations (a, b). We assumed that the persister cells mutated into resistant cells when the TKI treatment was initiated. The tumor growth models of Eqs. (4) to (6) that include seven parameters were simultaneously optimized using the Levenberg–Marquardt optimization method[18], which combined the Gauss–Newton algorithm and the gradient algorithm for nonlinear least squares curve-fitting problem (Supplementary Fig. S2). The optimization constraints were restrictions from 0 to 1 for initial fractions of persister and resistant populations, three cells population growth rates, and the mutation probability.

Seven reference TGT model parameters that were optimized by Levenberg–Marquardt method for each treatment were normalized, with the mean as 0 and standard deviation as ±1, before use as the training and test input of the TGT model:

$$params_{norm} = \left(\frac{2}{\underset{params}{max} - \underset{params}{min}} \right) \times params - \left(\frac{\underset{params}{max} + \underset{params}{min}}{\underset{params}{max} - \underset{params}{min}} \right) \quad (8)$$

where $params_{norm}$ was the value of the normalized parameters, $params$ was the original value of the referenced optimal parameters, and $\underset{params}{max}$ and $\underset{params}{min}$ were the maximum and minimum values, respectively, of the referenced optimal parameters.

Prediction of TGTs determined using a machine learning with imaging features

The pretreatment CT imaging features, which comprised tumor characteristics, were used for training the machine learning program, which determined the TGTs. In total, 486 image features were calculated based on 14 histogram-based and 40 texture-based features (Supplementary Table S5) for an original image and 8-wavelet-decomposition-filtered images. The texture-based features were calculated from the 4 texture characterization matrices of the gray-level co-occurrence matrix

(GLCM), gray-level run-length matrix (GLRLM), gray-level size-zone matrix (GLSZM), and the neighborhood gray-tone difference matrix (NGTDM). The 8-wavelet decomposition filters, that is, LLL, HLL, LHL, HHL, LLH, HLH, LHH, and HHH, contained the combinations of the low-pass filter (L) and high-pass filter (H) in three dimensions[19].

In each TKI group, the PCA was applied to 486 original image features using the function "sklearn.decomposition.PCA" in Python sklearn package for machine learning[20] in the training and test datasets to select three principal component features. The best combinations of first, first–second, and first–second–third principal component features were selected for each TKI by minimizing the RMSE between the predicted and referenced parameters value of TGT models.

Seven parameters of the TGT models were determined by two machine learning approaches, that is, SVR and RF, which learned the relationships between the principal component features and the reference parameters and were optimized by the Levenberg–Marquardt method.

The SVR, which uses a symmetrical loss function that equally penalizes high and low misestimates, is an effective tool in a real-value function estimation[21]. The optimal SVR parameters were obtained along with leave-one-out (LOO) cross validation to minimize the cost function, which was defined as:

$$Cost\ function\ = \left| N_{predicted} - N_{reference} \right| \tag{9}$$

where $N_{predicted}$ was the number of tumor cells predicted by the TGT model, and $N_{reference}$ was the number of tumor cells derived from CT images. Three SVR parameters were optimized by using the following ranges: 10^{-5} to 10 (step: 0.00001) for a gamma of the radial basic function (RBF); 1 to 10 (step: 1) for the regularization parameter C; and 10^{-3}, 10^{-2}, and 10^{-1} for an epsilon parameter. The function "sklearn.svm.SVR"[20] and "sklearn.model_selection.GridSearchCV"[22]

were used as the SVR model and the optimization tool of its parameters, respectively (Supplementary Fig. 3).

Furthermore, the RF[23] was employed to compare the prediction outcomes with SVR. All of the abovementioned input data settings were maintained for testing the robustness of each model. The function "sklearn.ensemble.RandomForestRegressor"[20] was used for the RF model with two parameters, which were also optimized using "sklearn.model_selection.GridSearchCV". Two RF parameters were optimized by using the following ranges: 1 to 100 (step: 1) for n_estimators (number of trees in the forest), and 1 to the maximum number of treatments minus 1 (step: 1) for max_depth (the maximum depth of the tree). The maximum value of max_depth was determined for each TKI group. The maximum values of max_depth were 6, 3, 7, and 7 for the afatinib, erlotinib, gefitinib, and osimertinib groups, respectively.

The RMSE between the predicted and referenced parameters value of TGTs model was calculated to optimize SVR parameters. Finally, the SVR models of four TKI groups were built and they were applied independently to the four test datasets.

Evaluation of proposed approach

The evaluation metrics in this study were a Spearman correlation coefficient and MAPE between the number of tumor cells derived from tumor volumes and the predicted number of tumor cells in the TGT model. The Spearman correlation coefficient evaluated the correlation between reference and predicted TGTs with the interpretation range[24] (Supplementary Table S6). In this study, the Spearman correlation coefficient could assess the tumor growth tendency, such as a transition from CR/PR to SD/PD.

The MAPE can evaluate the differences between the number of tumor cells derived from CT images and number of tumor cells predicted by the TGT model for training and test datasets at CT acquisition times. The equation for MAPE was defined as follows:

$$MAPE = \frac{1}{n} \times \sum_{i=1}^{n} \frac{\left| N_i^{predicted} - N_i^{reference} \right|}{N_i^{reference}} \times 100 \quad (10)$$

where n was the number of CT acquisition times, $N_i^{predicted}$ was the number of tumor cells predicted by the TGTs model, and $N_i^{reference}$ was the number of tumor cells derived from CT images. Then, the average MAPE was calculated among the four TKI groups to evaluate the overall prediction outcome.

Acknowledgments

This study was partially supported by a grant from Center for Clinical and Translational Research of Kyushu University Hospital and JSPS KAKENHI Grant Number 20K08084. We would like to give a warmly thank to all Arimura's laboratory members for giving comments to this study. Special appreciation for Department of Health Sciences, Kyushu University and MEXT Scholarship for providing author a great opportunity to perform advance medical research.

Author contributions

H.A. is a principal investigator, who has conducted this study. H.G.T. developed the model, calculated the data and wrote the manuscript. K.T., H.A., K.N. provided clinical knowledge for selecting the data and tumor segmentation, Q.C.L. helped in image features calculation. All authors contributed to build up the novel ideas and edited the manuscript.

Declarations of interest

None

References

1. Bray, F., Ferlay, J., Soerjomataram, I., Siegel, R. L., Torre, L. A., & Jemal, A. Global cancer statistics 2018: GLOBOCAN estimates of incidence and mortality worldwide for 36 cancers in 185 countries. *CA: a cancer journal for clinicians*, **68**(6), pp: 394-424, (2018).
2. Jorge, S. E. D. C., Kobayashi, S. S., & Costa, D. B. Epidermal growth factor receptor (EGFR) mutations in lung cancer: preclinical and clinical data. *Brazilian Journal of Medical and Biological Research,* **47**(11), pp. 929-939, (2014).
3. Solassol, I., Frédéric, P., and Xavier, Q. FDA-and EMA-Approved Tyrosine Kinase Inhibitors in Advanced EGFR-Mutated Non-Small Cell Lung Cancer: Safety, Tolerability, Plasma Concentration Monitoring, and Management. *Biomolecules*, **9**(11), pp. 668, (2019).
4. Michor, F., *et al*. A. Dynamics of chronic myeloid leukaemia. *Nature*, **435**(7046), pp. 1267-1270, (2005).
5. Foo, J. & Michor, F. Evolution of resistance to targeted anti-cancer therapies during continuous and pulsed administration strategies. *PLoS Comput Biol*, **5**(11), e1000557, (2009).
6. Mumenthaler, S. M. *et al.* The impact of microenvironmental heterogeneity on the evolution of drug resistance in cancer cells. *Cancer Informatics*, **14**, CIN-S19338, (2015).
7. Grassberger, C., *et al*. Patient-specific tumor growth trajectories determine persistent and resistant cancer cell populations during treatment with targeted therapies. *Cancer Research,* **79**(14), pp. 3776-3788, (2019).

8. Powerful combination therapies. *Nat Biomed Eng*, **2,** pp. 555–556, (2018). https://doi.org/10.1038/s41551-018-0283-1
9. Bitterman, D. S., & Du, K. L. Safety and Efficacy of Combination Targeted Therapy and Radiotherapy| PER. *American Journal of Hematology/Oncology®*, ***12***(1), (2016).
10. Herman, G. T., Zheng, J., & Bucholtz, C. A. Shape-based interpolation. *IEEE Computer Graphics and Applications*, **3,** pp. 69-79, (1992).
11. Hayes, S. A., *et al*. Comparison of CT volumetric measurement with RECIST response in patients with lung cancer. *European journal of radiology*, ***85***(3), pp. 524-533, (2016).
12. Schiavon, G., *et al*. Tumor volume as an alternative response measurement for imatinib treated GIST patients. *PloS one*, **7**(11), e48372, (2012).
13. RECIST version 1.1. *European Journal of Cancer,* **45**, pp. 228-247, (2009).
14. https://www.slicer.org. Accessed: 3 July 2020.
15. Benzekry, S. *et al*. Classical mathematical models for description and prediction of experimental tumor growth. *PLoS Comput Biol,* **10**(8), e1003800, (2014).
16. Simon E., Sebastien B. Mathematical modeling of tumor and metastatic growth when treated with sunitinib. *[Research Report] Inria Bordeaux Sud-Ouest*. hal-01377994, (2016).
17. Geng, C., Harald, P., & Grassberger, C. Prediction of treatment response for combined chemo- and radiation therapy for non-small cell lung cancer patients using a bio-mathematical model. *Scientific Reports,* **7**(1), pp. 1-12, (2017).
18. Arimura, H. *Image-based Computer-Assisted Radiation Therapy*. Singapore: Springer, (2017).
19. Soufi, M., Arimura, H. & Nagami, N. Identification of optimal mother wavelets in survival prediction of lung cancer patients using wavelet decomposition-based radiomic features. *Medical Physics,* **45**(11), pp. 5116-5128, (2018).

20. Pedregosa, F., *et al* Scikit-learn: Machine learning in Python. *The Journal of Machine Learning Research,* **12**, pp. 2825-2830, (2011).
21. Awad M., Khanna R. *Support Vector Regression. In: Efficient Learning Machines*. Apress, Berkeley, CA (2015). https://doi.org/10.1007/978-1-4302-5990-9_4
22. Paper, D. *Scikit-Learn Regression Tuning. In: Hands-on Scikit-Learn for Machine Learning Applications*. Berkeley, CA: Apress, (2020). https://doi.org/10.1007/978-1-4842-5373-1_7
23. Friedman, J., Hastie, T., & Tibshirani, R. *The elements of statistical learning* (Vol. 1, No. 10). New York: Springer series in statistics, (2001).
24. Mukaka, M. M. Statistics corner: a guide to appropriate use of correlation in medical research. *Malawi Medical Journal,* **24**(3), pp. 69-71, (2012).
25. Bethune, G., Bethune, D., Ridgway, N., & Xu, Z. Epidermal growth factor receptor (EGFR) in lung cancer: an overview and update. *Journal of Thoracic Disease,* **2**(1), pp. 48, (2010).
26. Brown, K., *et al*. Population pharmacokinetics and exposure-response of osimertinib in patients with non-small cell lung cancer. *British Journal of Clinical Pharmacology,* **83**(6), pp. 1216-1226, (2017).
27. Cohen, M. H., *et al*. United States Food and Drug Administration drug approval summary: gefitinib (ZD1839; Iressa) tablets. *Clinical Cancer Research,* **10**(4), pp. 1212-1218, (2004).
28. Cruz, J. A. & Wishart, D. S. Applications of machine learning in cancer prediction and prognosis. *Cancer Informatics*, **2**, 117693510600200030, (2006).
29. da Cunha Santos, G., Shepherd, F. A., & Tsao, M. S. EGFR mutations and lung cancer. *Annual Review of Pathology: Mechanisms of Disease,* **6,** pp. 49-69, (2011).

30. Eckstein, N., *et al*. Clinical pharmacology of tyrosine kinase inhibitors becoming generic drugs: the regulatory perspective. *Journal of Experimental & Clinical Cancer Research,* **33**(1), pp. 15, (2014).
31. Eisenhauer, E. A., *et al*. New response evaluation criteria in solid tumours: revised RECIST guideline (version 1.1). *European Journal of Cancer,* **45**(2), pp. 228-247, (2009).
32. Foo, J., Chmielecki, J., Pao, W., & Michor, F. Effects of pharmacokinetic processes and varied dosing schedules on the dynamics of acquired resistance to erlotinib in EGFR-mutant lung cancer. *Journal of Thoracic Oncology,* **7**(10), pp. 1583-1593, (2012).
33. Hata, A. N., *et al*. Tumor cells can follow distinct evolutionary paths to become resistant to epidermal growth factor receptor inhibition. *Nature Medicine,* **22**(3), pp. 262, (2016).
34. Herviou, P., *et al*. Therapeutic drug monitoring and tyrosine kinase inhibitors. *Oncology Letters,* **12**(2), pp. 1223-1232, (2016).
35. Jackman, D. M., *et al*. A phase I trial of high dose gefitinib for patients with leptomeningeal metastases from non-small cell lung cancer. *Oncotarget,* **6**(6), pp. 4527, (2015).
36. Kucharczuk, C. R., Alex, G., & Vozniak, J. M. Drug-Drug Interactions, Safety, and Pharmacokinetics of EGFR Tyrosine Kinase Inhibitors for the Treatment of Non–Small Cell Lung Cancer. *Journal of the Advanced Practitioner in Oncology,* **9**(2), pp. 189, (2018).
37. Miura, M. Therapeutic drug monitoring of imatinib, nilotinib, and dasatinib for patients with chronic myeloid leukemia. *Biological and Pharmaceutical Bulleti,* **38**(5), pp. 645-654, (2015).
38. Mizoguchi, K., *et al*. Pharmacokinetic parameters of gefitinib predict efficacy and toxicity in patients with advanced non-small cell lung cancer harboring EGFR mutations. *Cancer Chemotherapy and Pharmacology,* **78**(2), pp. 377-382, (2016).

39. Nishino, M., Jyothi, P. J., Nikhil, H. R., & Annick, D. V. D. A. Revised RECIST guideline version 1.1: what oncologists want to know and what radiologists need to know. *American Journal of Roentgenology,* **195**(2), pp. 281-289, (2010).

40. Nishino, M., *et al*. New response evaluation criteria in solid tumors (RECIST) guidelines for advanced non–small cell lung cancer: Comparison with original RECIST and impact on assessment of tumor response to targeted therapy. *American Journal of Roentgenology,* W **195**(3), pp. 221-228, (2010).

41. Nishino, M., *et al*. RECIST 1.1 in NSCLC patients with EGFR mutations treated with EGFR tyrosine kinase inhibitors: comparison with RECIST 1.0. *American Journal of Roentgenology, W* **201**(1), pp. 64-71, (2013).

42. Schmitt, M. W., Loeb, L. A., & Salk, J. J. The influence of subclonal resistance mutations on targeted cancer therapy. *Nature Reviews Clinical Oncology*, **13**(6), pp. 335-347, (2016).

43. Seto, T., *et al*. Erlotinib alone or with bevacizumab as first-line therapy in patients with advanced non-squamous non-small-cell lung cancer harbouring EGFR mutations (JO25567): an open-label, randomised, multicentre, phase 2 study. *The Lancet Oncology,* **15**(11), pp. 1236-1244, (2014).

44. Siah, K. W., Khozin, S., Wong, C. H., & Lo, A. W. Machine-Learning and Stochastic Tumor Growth Models for Predicting Outcomes in Patients with Advanced Non–Small-Cell Lung Cancer. *JCO Clinical Cancer Informatics*, **1**, pp. 1-11, (2019).

45. Simon, R. & Norton, L. The Norton–Simon hypothesis: designing more effective and less toxic chemotherapeutic regimens. *Nature Clinical Practice Oncology,* **3**(8), pp. 406-407, (2006).

46. Song, J., *et al*. A new approach to predict progression-free survival in stage IV EGFR-mutant NSCLC patients with EGFR-TKI therapy. *Clinical Cancer Research*, **24**(15), pp. 3583-3592, (2018).

47. Takeda, M., and Kazuhiko, N. First-and second-generation EGFR-TKIs are all replaced to osimertinib in chemo-naive EGFR mutation-positive non-small cell lung cancer? *International Journal of Molecular Sciences,* **20**(1), pp. 146, (2019).

48. Wind, S., Schnell, D., Ebner, T., Freiwald, M., & Stopfer, P. Clinical pharmacokinetics and pharmacodynamics of afatinib. *Clinical Pharmacokinetics,* **56**(3), pp. 235-250, (2017).

49. Werner, B., *et al*. The cancer stem cell fraction in hierarchically organized tumors can be estimated using mathematical modeling and patient-specific treatment trajectories. *Cancer Research*, **76**(7), pp. 1705-1713, (2016).

Figures

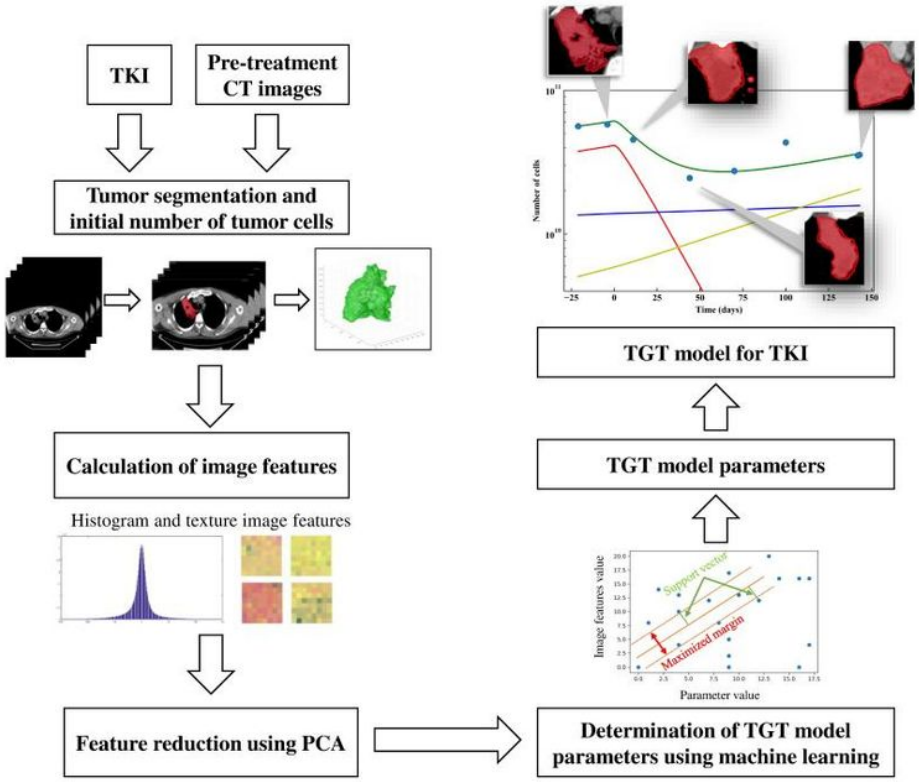

Figure 1

A scheme for the prediction of TGT models. TKI: tyrosine kinase inhibitor, PCA: principal component analysis, TGT: tumor growth trajectory.

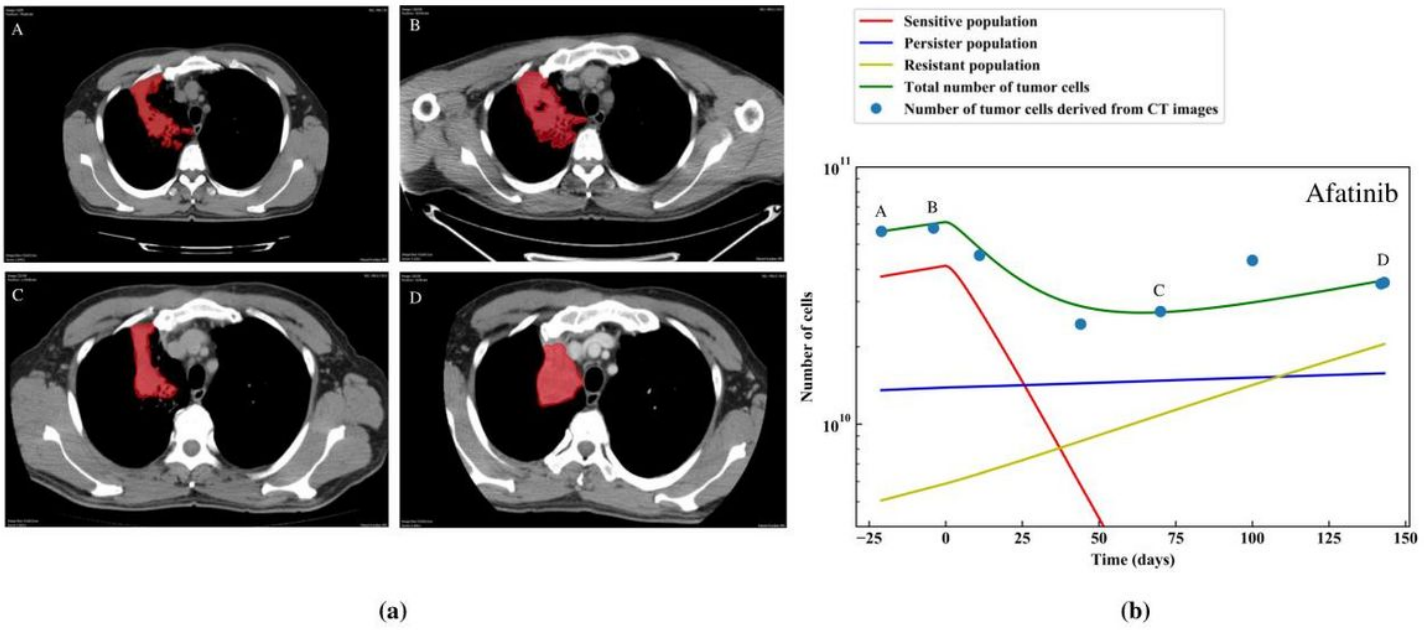

Figure 2

TGTs of a patient treated with afatinib in a test dataset: (a) actual lung tumor ROIs (red) on the pretreatment and follow-up CT images at four CT acquisition timepoints (A, B, C, and D) on the TGTs and (b) the predicted TGTs with the number of tumor cells derived from the CT images (solid circles).

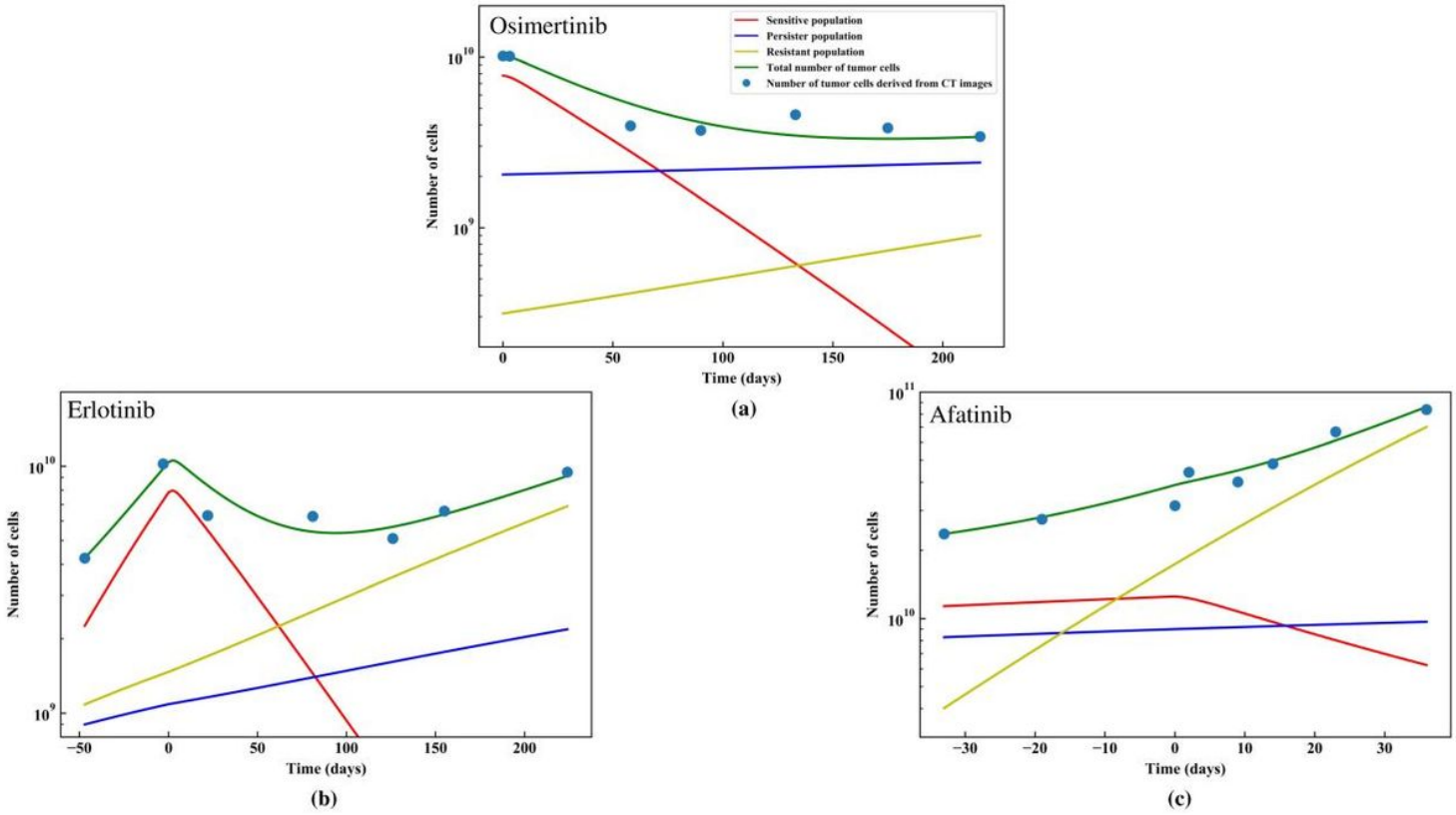

Figure 3

Three common types of TGTs: (a) PR to SD, (b) PR to PD, and (c) PD. PR: partial response, SD: stable disease, PD: progressive disease.

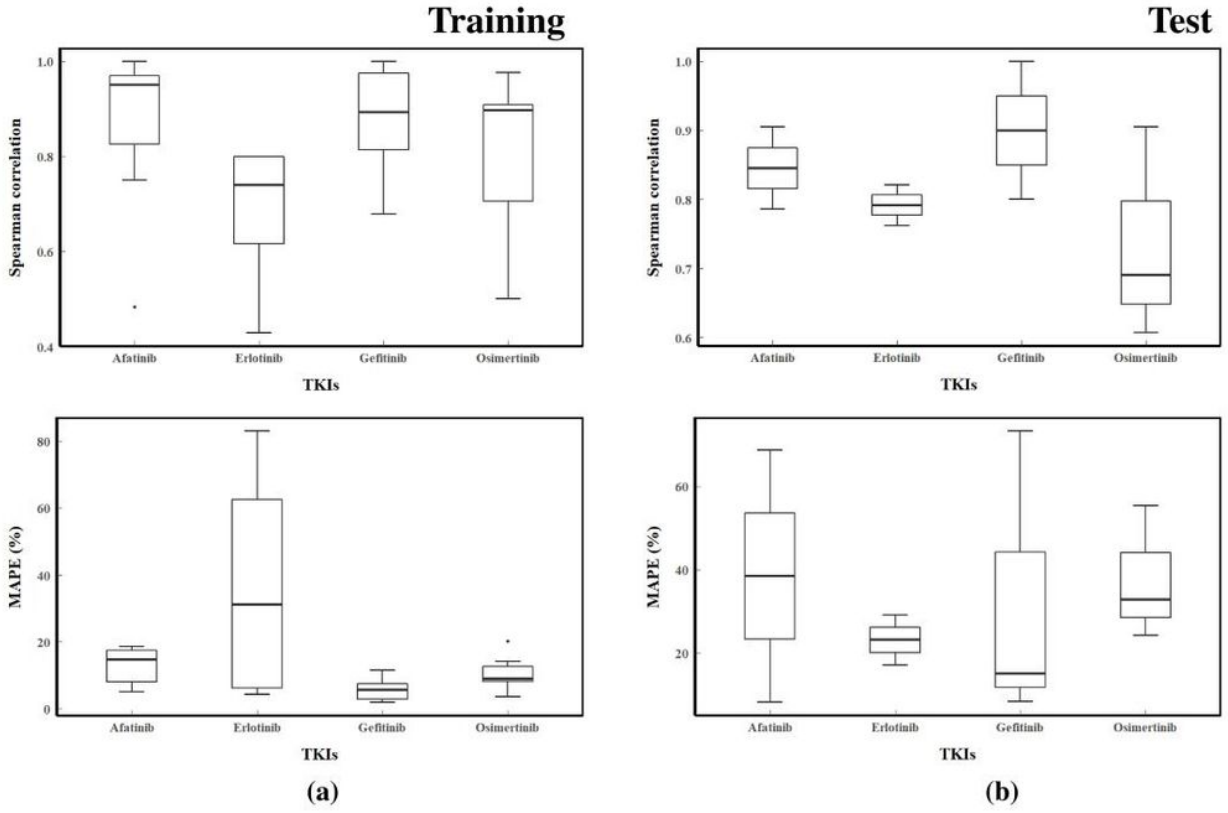

Figure 4

The box plot charts: (a) Spearman correlation and MAPE between the number of tumor cells derived from CT images and the number of tumor cells predicted by the TGT model in a training dataset; (b) Spearman correlation and MAPE between number of tumor cells derived from CT images and the predicted number of tumor cells estimated by a TGT model in a test dataset. TGTs: tumor growth trajectories, MAPE: mean absolute percentage error.

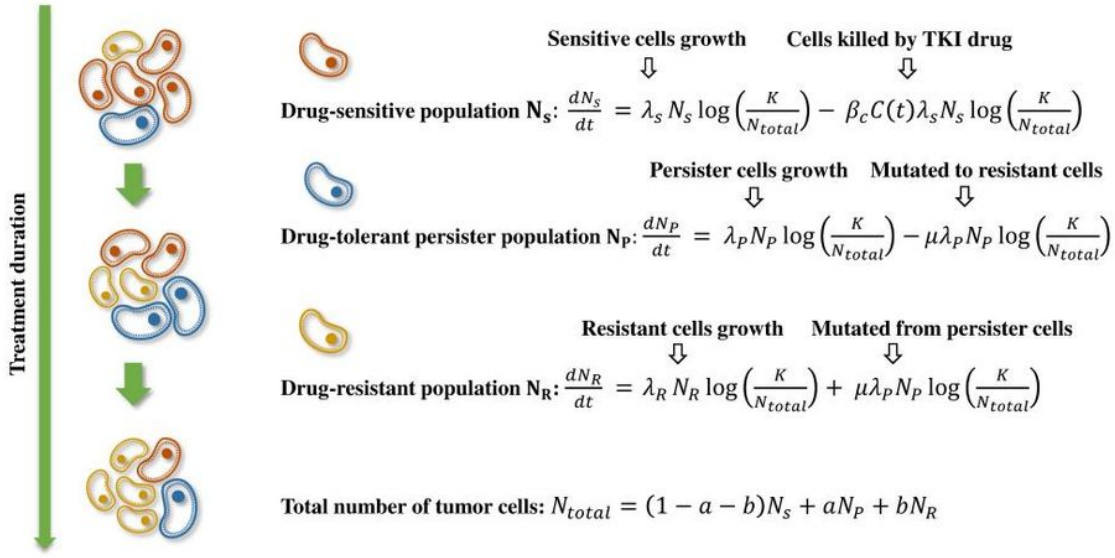

Figure 5

The TGT model of the time-variant number of tumor cells with the assumption that there are three components inside the NSCLC tumor: a drug-sensitive population, a drug-tolerant persister population, and a drug-resistant population

Supplementary Files

This is a list of supplementary files associated with this preprint. Click to download.

- TruongGiaHuySRSupplementaryFigures.pdf
- TruongGiaHuySRSupplementaryTables.pdf